BEAM ELEMENTS BASED ON A HIGHER ORDER THEORY-II. BOUNDARY LAYER SENSITIVITY AND STRESS OSCILLATIONS

G. Prathap,t$ R. U. **Vinayak** and **B. P. Naganarayana**
National Aerospace Laboratories, Bangalore 560017, India

(Received 30 June 1994)

Abstract-The flexure of deep beams and thick plates and shear flexible (e.g. laminated composite) beams and plates is often approached through a finite element formulation based on the Lo-Christensen-Wu (LCW) theory. A systematic analytical evaluation of beam elements based on the LCW higher order theory was carried out recently. It turns out that the availability of a large number of degrees of freedom to prescribe end/boundary conditions leads to discontinuity effects that trigger off wiggles (sharp oscillations) in some of the higher order displacement terms. These wiggles propagate outward from the point of excitation and disturb the transverse normal stress predictions. This paper examines the origin of these oscillations and how these boundary layer effects can be contained by refined modeling within the boundary layer zone or region when beam elements based on this higher order theory are used. A similar difficulty should be present in plate elements based on the same theory.

1. INTRODUCTION

For deep beams and thick plates and for beams and plates made of high-performance laminated composites, the classical theories based on the Kirchhoff-Love hypothesis no longer suffice. The Reissner and Mindlin theories provide a first-order improvement by accounting for the effects of transverse shear deformation and a very large number of papers based on these theories are available, see Part I of this paper [1] for a representative survey. A more refined theory which can better predict stresses through the thickness, e.g. inter-laminar stresses at boundaries, discontinuities etc. is provided by Lo, Christensen and Wu [2, 3] and has found much favor in finite element formulations-see Ref. [1] for a representative bibliography. This can now take into account transverse normal strain and stress effects and also allow for computation of interlaminar stresses by post-processing the FEM results using integration of equilibrium equations. Reference [1] gives a detailed description of the formulation and analysis of beam elements based on this theory.

Although the LCW theory has been widely used to develop beam and plate elements, the systematic analysis of how these elements behave in Ref. [1] revealed that the transverse normal stresses showed large oscillations near clamped boundary conditions. These oscillations became more violent as the beams become thinner. Further examination showed that some of the higher order degrees of freedom which are now available in the LCW theory to prescribe end/boundary conditions show sharp oscillations from node to node in the region where the boundary conditions are prescribed. This paper examines how discontinuity effects at the boundary trigger off such wiggles. These wiggles propagate outward from the point of excitation and disturb the transverse stress predictions. We shall now examine the origin of these oscillations and how these boundary layer effects can be damped out and contained by refined modeling within the boundary layer zone or region.

2. FINITE ELEMENT FORMULATION OF THE LO-CHRISTENSEN-WU (LCW) BEAM MODEL

Reference [1] describes in detail the finite element formulation of beam elements based on the LCW theory. As per LCW theory [2, 3], the inplane displacement field $u(x, z)$ is expanded as a cubic function in the thickness coordinate z. The corresponding polynomial expansion for transverse displacement w(x, z) is truncated at one order lower than the expansion for inplane displacement. This choice leads to a consistent definition of interpolation for the transverse shear strain with respect to the thickness coordinate z. Defining the displacement field in terms of the mid-surface degrees of freedom u_o, 0 wo, we write

$$u(x,z)=u_0(x)+zO,(x)+z^{z}uo(x)+z^{3}B^{*}(x) \qquad (1a)$$

$$w(x, z) = \text{w.}(x) + zO(x) + z^{2}\text{wo}(x). \qquad (1b)$$

The strain field associated with eqn (la) is

$$\frac{au}{ax} - \frac{au_{,}}{ax} + z\frac{ao_x}{ax} + z_2\frac{auo}{ax} + z^3\frac{M}{ax} \quad (2a)$$

$$\varepsilon_{ZZ} \quad az = B^z + 2zw_{\circ}^{*} \quad (2b)$$

$$\gamma_{xz} = \frac{au}{az} + \frac{aw}{ax} - 6^{x} + \frac{Ow,\sim}{a} + z\,2u_{0^*} + \frac{ae=1}{ax}$$

$$+z^2\ \underline{30^*+}\ \frac{14}{}). \quad (2c)$$

A two-noded linear element (BM2), three-noded quadratic element (BM3) and four-noded cubic element (BM4) have been developed for beams made of different isotropic and/or composite materials with fiber orientation angle of 0° with respect to x axis and layers stacked in z direction [1]. These elements have been systematically analyzed and the accuracy and other features of the computational model have been evaluated by comparing finite element method (FEM) results with available closed form elasticity solutions in Ref. [1]. Here, we are interested in the edge/boundary discontinuity effect and its influence on transverse normal stress predictions.

3. COMPUTATION OF TRANSVERSE STRESSES FROM INTEGRATION OF EQUILIBRIUM EQUATIONS

For the sake of completeness, we shall briefly discuss how the transverse stresses are evaluated. In the discussion that follows, we shall use d_x, *etc. to* denote stresses computed from the FEM solutions using the strain-displacement equations, eqn (2) and the constitutive law. Terms such as $Q_{x,\ T.,}$ denote stresses computed by integrating the equilibrium equations [see eqn (3) below]. The inplane stresses d_x can be accurately evaluated from the computed FEM nodal displacements $u_{\circ}$ to *wo* and the constitutive law and strain-displacement relation, eqn (2a). The FEM transverse stresses derived directly from the constitutive law and the strain displacement eqn (2b, c) using the same computed displacements are not very useful. One disadvantage is that the d, is accurate only to a linear order and $_{zfZ}$ is accurate only to a quadratic order through the thickness and these are therefore determined in a least-squares accurate sense of the actual strain, stress variation through the depth. Another difficulty is that transverse stresses have to be continuous across layer interfaces in the case of a beam made of many layers of different laminae, whereas transverse stresses derived from strains using eqn (2b, c) give discontinuous stresses if the layers have different elastic moduli. One can improve upon this by adopting a strategy based on integration of the equations of equilibrium for two-dimensional elasticity for each layer, and summing up over all layers to give a more accurate and realistic stress pattern. Thus, if we start with the bending stress d_x and transverse shear stress $_{ff,}$ which are computed from the FEM displacements using only the constitutive laws and strain displacement relations, we can compute improved $_{6Z}$ and T_x by using the relations

$$\frac{07_{S\cdot}}{az} - \frac{ao_x}{ax} \quad (3a)$$

$$\frac{aa_{=}}{az} - \frac{a\sim_{x\sim}}{ax} \quad (3b)$$

within each layer. Thus, after integration and evaluation of constants using an initial value problem strategy, one would get a quartic variation of $_{T.Z}$ and a cubic variation of $_{Qz}$ in the z direction. If we have $\varepsilon_{xz} = 0$ and $Q_{\prime} = 0$ at the bottom surface as the initial values, one should be able to get the correct values of ε_{xz} and $6,$ at the top surface, to an order of accuracy reflecting the accuracy inherent in the computation of stresses such as d_x and ε_{xZ} in the FEM solution process. We found that these accuracies were maintained when we carried out the finite element experiments [1].

4. ANALYTICAL PREDICTIONS FOR NUMERICAL EXPERIMENTS

The plane stress solution using the Airy stress function approach for a laterally loaded isotropic cantilever beam by Venkatraman and Patel [4] provides a useful bench-mark solution for evaluating the accuracy and efficiency of our present finite element models (see also Ref. [1]). For the configuration shown in Fig. 1, we obtain the following expression for the stress a,

$$a,= -(p/1201)[5(-4z^3 + 3h^2z + h^3)] \quad (4)$$

when the beam is of rectangular cross-section of unit width and depth *h,* so that $I = h'1\,12$, and is loaded by a uniformly distributed load of intensity p = 1.0 on the top surface, z = h/2. If we recast eqn (4) in terms of a dimensionless co-ordinate $q = 2z/h,$ we have

$$QZ=-P[(l+n)/2-n(n2-1)/4]. \quad (5)$$

z,,

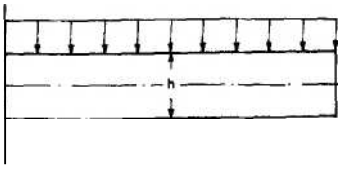

Fig. 1. Laterally loaded isotropic cantilever.

Another set of results we shall need are least squares fit approximations of the functions for a, we have in eqn (5). We now know that finite element displacement method solutions seek strains/stresses in a least squares accurate sense [5]. Thus strains/stresses computed directly from the FEM displacement fields using the strain-displacement and stress-strain matrices, would be obtained as least squares accurate approximations of the actual state of stress. It will therefore be interesting at this stage to predict what the least-squares accurate fit up to linear order through the thickness are for a_z from eqn (5), so that this can be compared with d the FEM solutions determined using eqn (2b) and the computed displacements fields. It can be shown that the least squares approximations a, (Is) for the case where the load is applied on z = h /2 is

$$a\text{-}(Is) = -p(1/2+3x1/5). \qquad (6)$$

5. NUMERICAL EXPERIMENTS

So far, we have set the stage for the evaluation of the transverse normal stress from finite elements based on the higher order LCW theory by deriving *a priori* analytical estimates for their behavior. We shall now confirm the validity of these predictions by performing carefully chosen numerical experiments.

A thin cantilever beam (1 = 10.0, h = 1.0) and a deep beam (*l = h* = 10.0) are considered for numerical studies. Young's modulus, E = 1000.0, Poisson's ratio, v = 0.0 and uniformly distributed load p = 1.0 applied on the top surface are assumed. All the degrees of freedom available at the root (i.e. at x = 0) are suppressed. A uniform mesh of 10 elements is used unless otherwise specified.

5.1. *Transverse normal stresses in thin beams*

Figure 2 depicts the distribution of transverse normal stress o . at x = 5.5 (centroid of the sixth element from the root, in a 10 element uniform mesh) for a thin beam. The variation of a, computed by FEM using the equilibrium eqn (3b), agrees very well with the a, distribution obtained by the Venkatraman and Patel solution, eqn (5). Also shown in Fig. 2 are the results obtained from a three-dimensional model using eight-noded brick elements from three-dimensional-FEES, an inhouse package developed at NAL [6]. An accurate representation is achieved here-in fact 24 brick elements are used through the depth of the beam and the symbols in Fig. 2 are placed at element centroids where the stresses are obtained most accurately. We see here that for a thin beam, both the LCW and Venkatraman and Patel solutions are very close to each other and to the three-dimensional FEM model results.

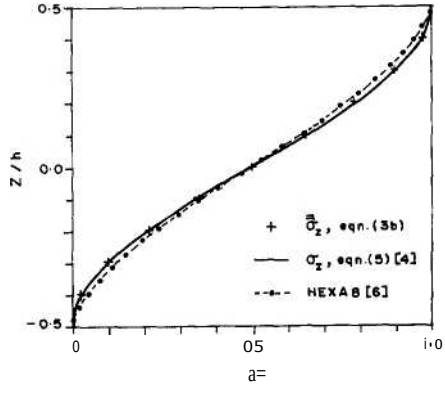

Fig. 2. a, pattern in thin beam *(1/h = 10),* at x = 5.5.

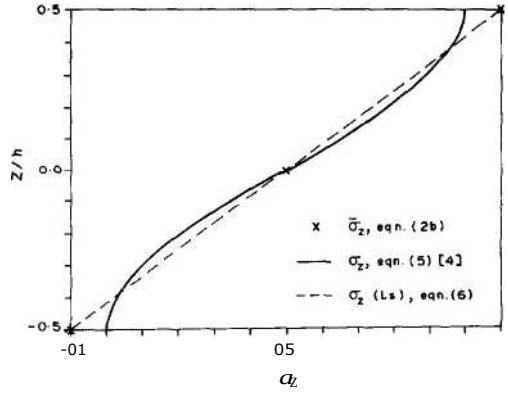

Fig. 3. a pattern in thin beam *(1/h = 10),* at *x* = 5.5, least squares interpretation.

Figure 3 shows the least squares fit interpretation of the present results. We see that the distribution of d, [evaluated using the FEM displacements and eqn (2b)] is in exact agreement with the least squares fit distribution a,(ls) of Venkatraman and Patel's solution, eqn (6). This is also seen to be the least squares fit of both a, and a=. This is in line with the understanding that finite element displacement method solutions seek strains/stresses in a least squares accurate sense [5].

Next we consider the distribution of a, for the same thin beam at the section x = 0.5, which is the centroid of the element placed at the root where the clamped boundary conditions are enforced by suppressing all seven degrees of freedom. From Fig. 4 we see that a,

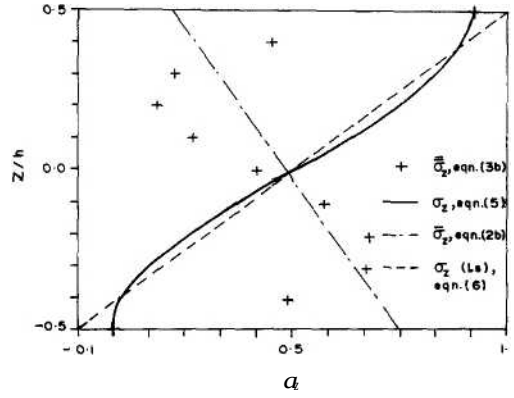

Fig. 4. a, pattern in thin beam *(l/h = 10),* at x = 0.5.

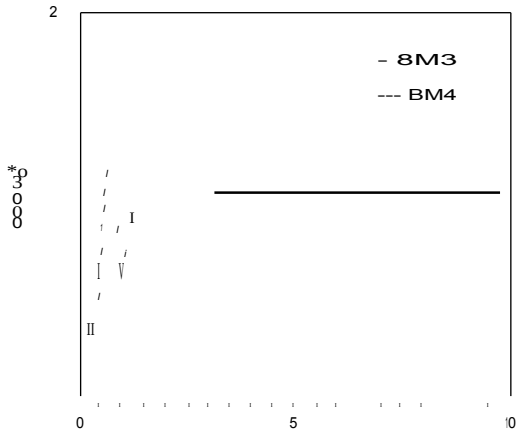

Fig. 5. Variation of wo along length of thin beam (1/h = 10).

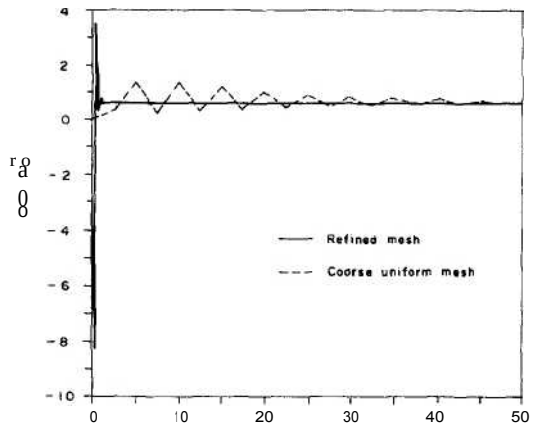

Fig. 7. Variation of w_0^* along length of very thin beam (11h = 50).

starts from zero at z = -h/2 = -0.5 and reaches p = 1.0 at z = h12 = 0.5 which is the applied load on the top. However, a large oscillation is seen in Q_j--the significant differences between σ_z and v_z are obvious. Similarly, 6,, is completely different from σ_z (ls), the former appearing to be a least squares fit of $_{7T,}$

These discrepancies can be attributed to the disturbances on the higher order displacement terms for an element at the root during the fem solution. When we take a close look at the variation of the higher order displacement terms predicted by the FEM solution, some interesting facts are seen for w_0^* and 0_. In Fig. 5 we notice very large wiggles in wo triggered off at x = 0 which gradually die down as we go away from the root. Again, near the tip, wo shows oscillations, which however, are much smaller in comparison to those near the root and these die down more quickly. Similarly, 0, shows very small oscillations only near the root and these die down very rapidly (Fig. 6). In both Figs 5 and 6 we notice that the magnitude of oscillations in wo and 0, near x = 0 from BM4 elements are larger in comparison to that of BM3 elements; however, these oscillations damp down faster in BM4 elements. This, as we shall see again in our experiments to follow, is due to the presence of more nodes in BM4 elements than in BM3 elements for the same length of the beam, which enables the BM4 elements to capture the edge/boundary discontinuity effects more efficiently.

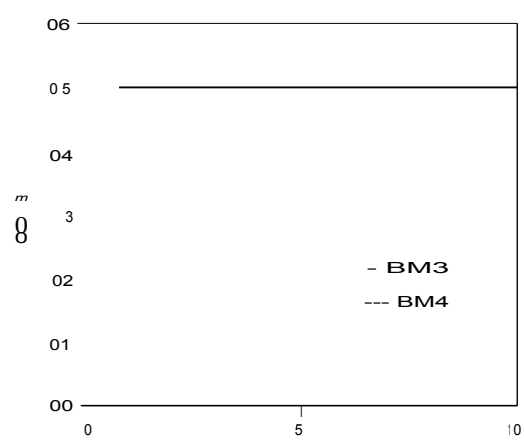

Fig. 6. Variation of 0, along length of thin beam (1/h = 10).

The disturbances near the tip due to the free boundary effects, though present, are too small in comparison to those near the root (see Fig. 5). This implies that the effect of the free boundary is much less on the displacement field.

Figure 7 shows the variation of wo along the length of a very thin beam of dimensions 1= 50.0, h = 1.0 carrying a uniformly distributed load p = 1.0 on top. In the case of the uniform mesh, 10 elements of equal length are used while for the refined mesh the first 10 elements from the root are of length 0.5 each and the remaining 9 elements are of length 5.0 each. We see from Fig. 7 that in the uniform mesh model, oscillations in wo are triggered off at x = 0 and persist until the tip, although there is a gradual decrease in their amplitude. The refined mesh (i.e. with small elements in the boundary layer region) results show oscillations of much greater amplitude very close to the root (the maximum absolute amplitude is 8.318828×10^{-3} as compared to the maximum amplitude of 1.350447×10^{-3} in the uniform mesh results), but they die down very rapidly (at x = 1.5, these oscillations are negligible). Experiments on graded meshes with elements of varying sizes in the boundary layer zone showed that the oscillations are chaotic in nature and no meaningful predictions could be made in this zone. However, it was also clear that the smaller the size of the elements used in the boundary layer zone, the more efficiently the oscillations are filtered out within this zone, leaving a large region where the FEM results for displacements and stresses could be reliably used. The boundary layer seems to be in the region of *h* to 1.5h for the present example.

We now go back to the thin beam of dimensions *I = 10.0, h = 1.0* loaded on top but use a refined mesh of 10 equal length elements in the first unit length

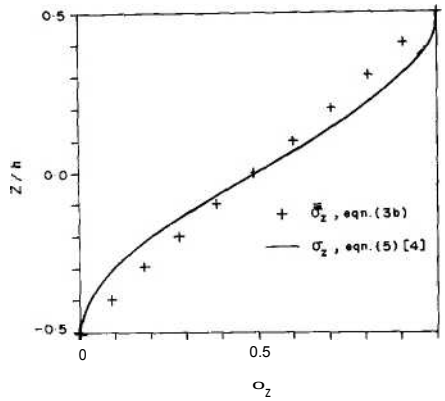

Fig. 8. *a,* pattern in thin beam *(1/h = 10),* at $x = 0.55$, using refined mesh.

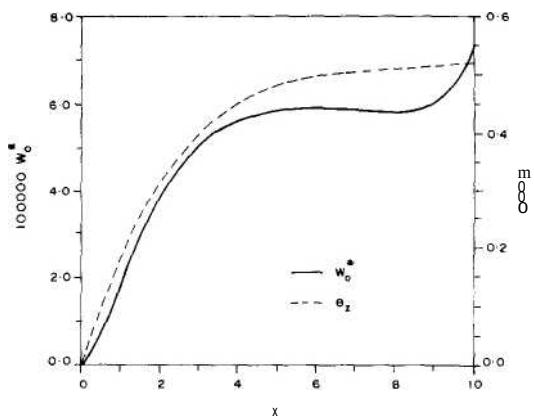

Fig. 10. Variation of wo and 0. along length of deep beam *(1/h = 1).*

from the root. Q_z at x = 0.55 in this case changes monotonically from 0 at the bottom to 1.0 at the top (see Fig. 8) unlike in Fig. 4 where we saw a large oscillation in σ_i at $x = 0.5$ when a single element was used in the first unit length from the root. This stress pattern however, is predominantly linear near the root, unlike the Venkatraman and Patel solution which shows a cubic variation for a,. The oscillations in the higher order terms also die down much faster when we use the refined mesh (results not presented).

5.2. *Transverse normal stresses in deep beams*

So far we have talked about the distribution of a, in a thin beam. To obtain further insight into the problem, we shall now take up the case of the deep beam. We use a uniform mesh of 10 elements. At x = 5.5, far from the boundaries, 6, and 8_z match closely a. and a,(ls), respectively (results not presented). For a section at x = 0.5, close to the root of a deep beam carrying a uniformly distributed load on top, we see from Fig. 9, fluctuations in a, which starts from zero at $z = -h/2 = -5.0$ and reachesp = 1.0 at $z = h/2 = 5.0$. Even a graded mesh of 18 BM3 elements (very small elements at the fixed and free ends and larger elements elsewhere) predicts a stress pattern which is very close to the uniform 10 element distribution (result not presented). The three-dimensional-FEES solution predicts very low and almost a constant transverse normal stress for $z/h = -0.45$-0.3 which steeply ascends top = 1.0 at z/h = 0.5. The present and the three-dimensional-FEES results are close to each other near $z = h/2$. The Venkatraman and Patel solution shows a stress pattern which is the same as in the case of the thin beam (see Fig. 4) and this pattern is very much different from the present and the three-dimensional-FEES results. Clearly, the Venkatraman and Patel solution is unreliable for deeper beams. Unlike in the thin beam, the variations of wo and 0, along the length (Fig. 10) do not show any wiggles or oscillations (both the uniform and the graded mesh yield identical patterns). Therefore the differences in the transverse normal stress distributions between the present and the three-dimensional-FEES results seem to be due to the limitations of the LCW formulation near the fixed end of the beam loaded on the top surface as the beam depth becomes large.

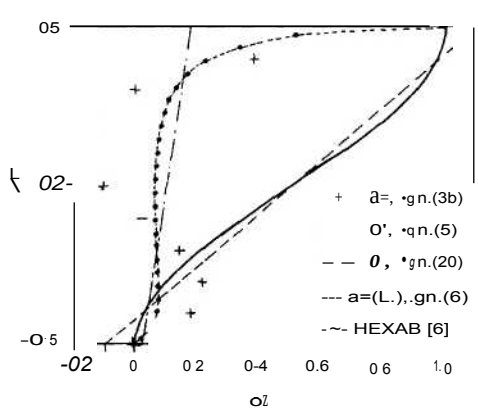

Fig. 9. *a* pattern in deep beam *(1/h = 1),* at x = 0.5.

5.3. *Mechanism triggering wiggles and stress oscillations*

From the studies of very thin, thin and deep beams, and with particular reference to Figs 4 and 9, it is possible to deduce how the transverse normal stresses develop from the near-field to the far-field from the point where the clamped boundary condition is applied-see Fig. 11. It's clear that elements placed far away $(x >> h)$ from the point where the clamped boundary condition is imposed are able to capture the developed stress pattern easily. However, an element placed near the root (i.e. $x << h$ in Fig. 11) would respond by showing large oscillations in stresses and the displacement terms are correspondingly disturbed to reflect these. This picture was confirmed in Fig. 9.

It is easy now to establish the probable mechanism triggering these oscillations. At x = 0, we have c, = 0 along z due to the imposition of the clamped boundary conditions whereby all the degrees of freedom at the root are suppressed. However, immediately in its

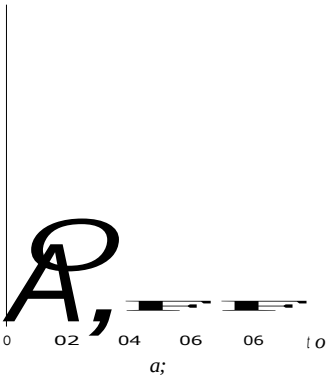

Fig. 11. a_{-} pattern in near field (typically $x << h$) and far-field ($x >> h$) from clamped end.

neighborhood, i.e. x > 0, we need a finite and non-zero value of $E_{,,}$ which in a little distance from the root will fully develop to the value of C, given by eqn (5). The first element, which has one node at the root, will be unable to account for this sudden jump that triggers off the oscillations. Also, it can be argued that a- will fully develop to the variation described by eqn (5) only at a small distance from the clamped node. There will therefore be a small boundary layer region near such discontinuities where the effect of the jump will be felt in a finite element model. Thus, an accurate analysis can be performed only by choosing graded meshes which permit considerable refinement (i.e. very small elements) in the boundary layer region.

Our experiments also gave useful guidelines to determine how the boundary layer effect manifests itself; experience with related phenomena in fluid flow modeling, especially in regions where discontinuities appear (e.g. modeling of shocks), indicate that the boundary layer length will be of the order of the beam thickness h (for a beam of length !) and that very small elements must be used in the jump region to remove the oscillations fast. The results of our numerical computations (compare Figs 5, 7 and 10) establish this nature.

These studies lead us to the conclusion that the edge/boundary/discontinuity effects cause the oscillations and wiggles in wo and B, and that they are dependent on the dimensions of the beam and the finite element size used in the boundary layer-zone. Further, the disturbances in the stress pattern near the root result from these edge/boundary/discontinuity effects. One should exercise extra care in modeling the boundary layer region. This zone must contain elements sufficiently small to restrict the boundary effects to a very short length so that the FEM results are reliable elsewhere. However, the results in this zone will be very erratic.

6. CONCLUSIONS

The effectiveness and the accuracy of the finite element beam model based on the higher order LCW theory is studied closely. The edge/boundary and discontinuity effects on the displacement and stress fields are investigated.

The stress predictions in thin and deep isotropic cantilever beams are accurate at points far from the boundaries, but become inaccurate near the root, in the case of the thin beam, when a coarse mesh is used. These discrepancies are caused by the disturbances in the higher order displacement terms for an element at the root, which in turn originate as a result of the edge/boundary discontinuities. Studies show that there is a boundary layer adjacent to the region where discontinuities appear and that very small elements must be used in this region to remove the oscillations fast. The greater the number of elements in the boundary layer, the greater the amplitude of the oscillations in the higher order displacement terms, and the faster the decay in these displacement terms. The effect of the free boundary on the displacement and stress fields is much less in comparison to that of the fixed boundary. The wiggles and oscillations in the higher order displacement terms are also dependent on the dimensions of the beam, i.e. the thinner the beam, the larger the oscillations and wiggles in these terms.

It is expected that a similar effect should be present when plate elements based on LCW theory are used. Figure 12 of Ref. [7] shows such a pattern for the transverse normal stress on the edge of a plate. Thus, if care is taken in using refined modeling in the boundary layer zone or strips, it can be concluded that the LCW theory is well suited for the formulation of beam and plate elements for stress analysis of layered composite structures.

Acknowledgements-The authors acknowledge the encouragement and support from Dr K. N. Raju, Director and Dr B. R. Somashekhar, Head of the Structures Division, N.A.L., Bangalore.

REFERENCES

1. R. U. Vinayak, G. Prathap and B. P. Naganarayana, Beam elements based on a higher order theory-I. Formulation and analysis of performance. *Comput. Struct.* ***58,*** 775-789 (1996).
2. K. H. Lo, R. M. Christensen and E. M. Wu, A higher order theory for plate deformations, Part l: homogeneous plates. *J. appl. Mech.* ***44,*** 663-668 (1977).
3. K. H. Lo, R. M. Christensen and E. *M. Wu,* A higher order theory for plate deformations, Part 2: laminated plates. *J. appl. Mech.* ***44,*** 669-676 (1977).
4. B. Venkatraman and S. A. Patel, *Structural Mechanics with Introduction to Elasticity and Plasticity*. McGraw-Hill, New York (1970).
6. G. Prathap, *The Finite Element Method in Structural Mechanics.* Kluwer Academic Press, Dordrecht (1993).
6. G. Prathap and B. P. Naganarayana, 3D-FEES-theoretical manual. PD ST 9005, N.A.L. Bangalore, India (1990).
7. J. J. Engblom and O. O. Ochoa, Through the thickness stress predictions for laminated plates of advanced composite materials. *Int. J. numer. Meth. Engng 21,* 1759-1776 (1985).